

# Atomic composition/configuration dependent bulk moduli of Al-C composites

Cite as: AIP Advances **12**, 115008 (2022); <https://doi.org/10.1063/5.0117900>

Submitted: 08 August 2022 • Accepted: 11 October 2022 • Published Online: 04 November 2022

 Hansika I. Sirikumara, Wilson Rativa-Parada, Robinson Karunanithy, et al.



View Online



Export Citation



CrossMark



# Atomic composition/configuration dependent bulk moduli of Al–C composites

Cite as: AIP Advances 12, 115008 (2022); doi: 10.1063/5.0117900

Submitted: 8 August 2022 • Accepted: 11 October 2022 •

Published Online: 4 November 2022



View Online



Export Citation



CrossMark

Hansika I. Sirikumara,<sup>1,a)</sup>  Wilson Rativa-Parada,<sup>2</sup> Robinson Karunanithy,<sup>3</sup> Poopalasingam Sivakumar,<sup>3</sup>   
Sabrina Nilufar,<sup>2,b)</sup> and Thushari Jayasekera<sup>3</sup> 

## AFFILIATIONS

<sup>1</sup>E. S. Witchger School of Engineering, Marian University Indianapolis, Indianapolis, Indiana 46222, USA

<sup>2</sup>School of Mechanical, Aerospace, and Materials Engineering, Southern Illinois University Carbondale, Carbondale, Illinois 62901, USA

<sup>3</sup>School of Physics and Applied Physics, Southern Illinois University Carbondale, Carbondale, Illinois 62901, USA

<sup>a)</sup> Author to whom correspondence should be addressed: [hsirikumara@marian.edu](mailto:hsirikumara@marian.edu)

<sup>b)</sup> Electronic mail: [sabrina.nilufar@siu.edu](mailto:sabrina.nilufar@siu.edu)

## ABSTRACT

Embedding carbon in metals has long been known to enhance the mechanical properties of metal carbon composites. We report the possibility of growing Al–C composites by the hot isostatic pressing method, with carbon embedded into an Al lattice in graphitic form without the formation of Al<sub>4</sub>C<sub>3</sub>. Raman spectroscopy confirms the formation of sp<sup>2</sup>-hybridized carbon clusters in the aluminum lattice. The bulk moduli of the samples were measured to be between 60 and 100 GPa. From the results of first principles density functional theory calculations, we show that the formation of sp<sup>2</sup>-hybridized carbon clusters is more stable than having isolated C scatterers in aluminum. Our results show that the extended network of C clusters shows a higher bulk modulus while isolated scattering centers could lower the bulk modulus. We explain this behavior with the analysis of total charge distribution. Localization of charge density decreases materials' ability to respond to external stress, thus showing a reduced bulk modulus. Some defect configuration may reduce the symmetry while others keep the symmetry of the host configuration even for the same chemical composition of Al–C composites.

© 2022 Author(s). All article content, except where otherwise noted, is licensed under a Creative Commons Attribution (CC BY) license (<http://creativecommons.org/licenses/by/4.0/>). <https://doi.org/10.1063/5.0117900>

Aluminum (Al) and its alloys are of interest because of their significant role in applications requiring lightweight yet strong materials utilized in the building of infrastructure such as transmission of electricity in high-voltage power lines, fabrication of high performance electronics, and construction of lightweight aerospace, naval, and automotive vehicles. Several strengthening techniques have been employed in the development of Al alloys and composites, such as solid solutions, precipitation strengthening, etc.<sup>1</sup> Aluminum matrix composites based on particulate reinforcement provide an excellent approach to improve the mechanical properties, with a combination of high specific strength, high stiffness, and lightweight.<sup>2,3</sup> Various ceramic reinforcements, such as SiC, B<sub>4</sub>C, TiC, Al<sub>2</sub>O<sub>3</sub>, and different carbon allotropes, are commonly used in the manufacturing of discontinuously reinforced Al matrix composites.<sup>4</sup> Graphene, a carbon allotrope, is used as the reinforcement in this study. In the process of incorporating carbon into the Al matrix,

it is important to limit the formation of Al<sub>4</sub>C<sub>3</sub> while preserving the sp<sup>2</sup> bonding network of carbon.

In this work, we report the fabrication of the Al–C composite with a graphitic network of carbon by the hot isostatic pressing method. Raman spectroscopy confirms the formation of sp<sup>2</sup> hybridized graphitic networks in Al. Our mechanical strength measurements show a bulk modulus in the range of 60–100 GPa in Al–C composites. Using the results from first principles Density Functional Theory (DFT) calculations, we explore the reasoning for such variation in the bulk modulus of Al–C composites at the atomistic level. Formation of a graphene sheet on the Al(111) surface has been previously studied by various groups.<sup>5–7</sup> However, the formation of C islands within the Al matrix has not been studied yet. In this work, we will discuss the bulk modulus of Al–C composites with C scatterers and sp<sup>2</sup>-hybridized graphitic C islands in the Al matrix. Our results suggest that C scatterers in the Al matrix will

result in localization of the charge density, thus decreasing the bulk modulus. An extended network of C in Al will preserve the uniform charge distribution, which will result in an increase in the bulk modulus.

Here, we explain the methodology for sample preparation, characterization of samples with Raman spectroscopy, measurement of the bulk modulus, and the detailed computational approach for calculating the bulk modulus of Al–C composites using first principles Density Functional Theory (DFT).

Al 6061 powder used as the base material (mesh size: –140/+325) was obtained from READE Advanced Materials. Graphene nanoplatelets with an average thickness of 2–8 nm, an average number of layers of 3–6, and 99.5+% purity were obtained from US Research Nanomaterials Inc. Both Al 6061 neat- and Al 6061-graphene composites were produced by powder metallurgy. The composites were mechanically milled using a SPEX 8000 mixer (SPEX corp.) for 4 h, with 1 wt. % of stearic acid [CH<sub>3</sub>(CH<sub>2</sub>)<sub>16</sub>COOH] obtained from Sigma-Aldrich (95%) used as a lubricant agent. The stearic acid was evaporated for 30 min at 450 °C before pressing. Hot isostatic pressing was used to consolidate the mechanically milled powder composites with 0.5 and 1 volume fractions of graphene reinforcement. The mixed powder was placed in a graphite die with a diameter of 25.4 mm and pressed for 1 h at 500 °C and 70 MPa under vacuum conditions in a front-loading hot press furnace (Materials Research Furnaces Inc.).

A Horiba iHR550 imaging spectrometer with a near-infrared (NIR) excitation light source at a wavelength of 785 nm (iBeam-Smart-785-S-WS, TOPTICA Photonics) was utilized for the Raman study. The system is equipped with an Olympus BX 41 microscope with 10×, 20×, 50×, and 100× magnification objectives. A grating of 600 gr/mm was used in the spectrometer. Except for carbon powder samples, the spectra were collected at 10× magnification at 120 mW laser power with 15-s acquisition time, and a total of ten scans were obtained over the desired range. The 100× objective with 10 mW laser power was used for carbon powder samples to avoid burning the samples.

Compressive tests were performed according to the standard ASTM E9 at room temperature in an MTS Insight 30 kN testing machine with a constant crosshead speed of 0.05 mm/min. The samples were machined to rectangular shapes with a length/width ratio of 2:1. Three samples of each composite material (neat, 0.5 and 1 vol. % of graphene) were tested in accordance with the ASTM E9 standard.

The bulk modulus of a system is defined as

$$B = -V \frac{dP}{dV},$$

which can be calculated with the equation of state, the relationship between the volume ( $V$ ) of a material and its pressure ( $P$ ).<sup>8</sup> In this work,  $B$  is calculated using by fitting the energy–volume curve to the Murnaghan equation of state,

$$P(V) = \left( \frac{B}{B'} \right) \left[ \left( \frac{V_0}{V} \right)^{B'} - 1 \right],$$

which assumes a linear behavior for the bulk modulus with respect to pressure.<sup>9</sup> Here,  $B$  is the bulk modulus, and  $B'$  is the first derivative

of the bulk modulus. The corresponding pressure ( $P$ ) can also be written as  $P = -\frac{dE}{dV}$ .

In order to extract the value of the bulk modulus,  $B$ , we calculated the energy of the Al–C composites for a series of lattice constants around the equilibrium lattice constant and then fitted it to the Murnaghan equation of state through implementation in the *ev.x* code in the Quantum Espresso (QE) package.<sup>10</sup>

Aluminum (Al) crystallizes in an FCC structure with a lattice constant of 4.04 Å. There are four atoms in a non-primitive cubic unit cell. In the present work, we considered a  $2 \times 2 \times 2$  supercell of aluminum with 32 atomic sites. This super cell allows us to study the 3.125% of C in aluminum, where only one out of 32 Al atoms is substituted with C. We considered three types of C dopants in Al: pure substitutional, pure interstitial, and mixture of substitutional/interstitial dopants. Our calculation cell with the composition Al<sub>(32– $n$ )</sub> C <sub>$m$</sub>  is denoted as C <sub>$m$</sub>  <sup>$n$</sup> , for which  $n = m$  is a purely substitutional configuration.

All energy values for this study were calculated using first principles Density Functional Theory (DFT) through implementation in the Quantum Espresso (QE) package.<sup>11</sup> The Generalized Gradient Approximation of Perdew, Burke, and Ernzerhof (GGA-PBE) was used for the exchange and correlation functionals with a 40 Ry energy cut-off for plane wave expansion.<sup>12</sup> A  $12 \times 12 \times 12$  Monkhorst–Pack grid was used to sample the Brillouin zone, and all the structures were optimized to forces less than 0.025 eV/Å.

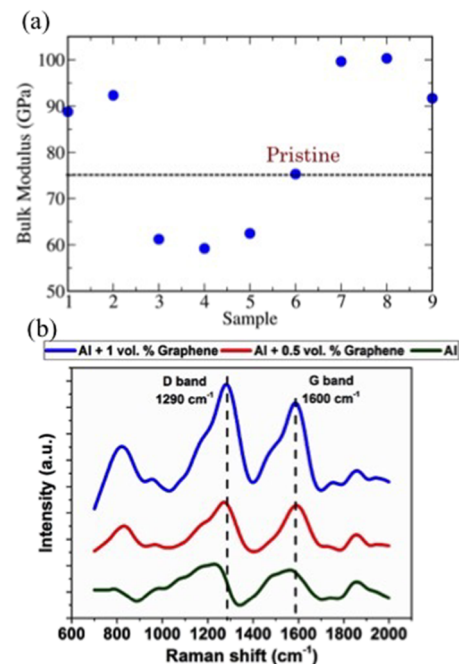


**FIG. 1.** (a) Upper panel shows the experimentally measured bulk modulus of nine samples of Al and Al–C composites, and (b) the lower panel shows the Raman spectra obtained for Al with no carbon in comparison with the two samples of the Al–C composite.

In order to get a deeper understanding on the relation between the change in the bulk modulus and the atomic configuration, we analyzed the charge density distribution of each system. Charge density is an indicator of the symmetry of the system. Once the symmetry is broken, it has the ability to respond to the reduction in the external force, thus reducing the bulk modulus. We also calculated gamma-point phonon frequencies of the selected Al-C composites to further understand the nature of bonding, which was also observed through Raman spectroscopy. The phonon frequencies were calculated using density functional perturbation theory through implementation in the Quantum Espresso package.

Measurements of the bulk modulus for nine samples show a variation from 60 to 100 GPa, as shown in the upper panel of Fig. 1. These nine samples have three different chemical composites. The compressive modulus is determined for three samples of each kind, namely, neat Al and 0.5 and 1 vol. % graphene reinforced Al. The experimental modulus shows scattered results for different samples for the same chemical composition.

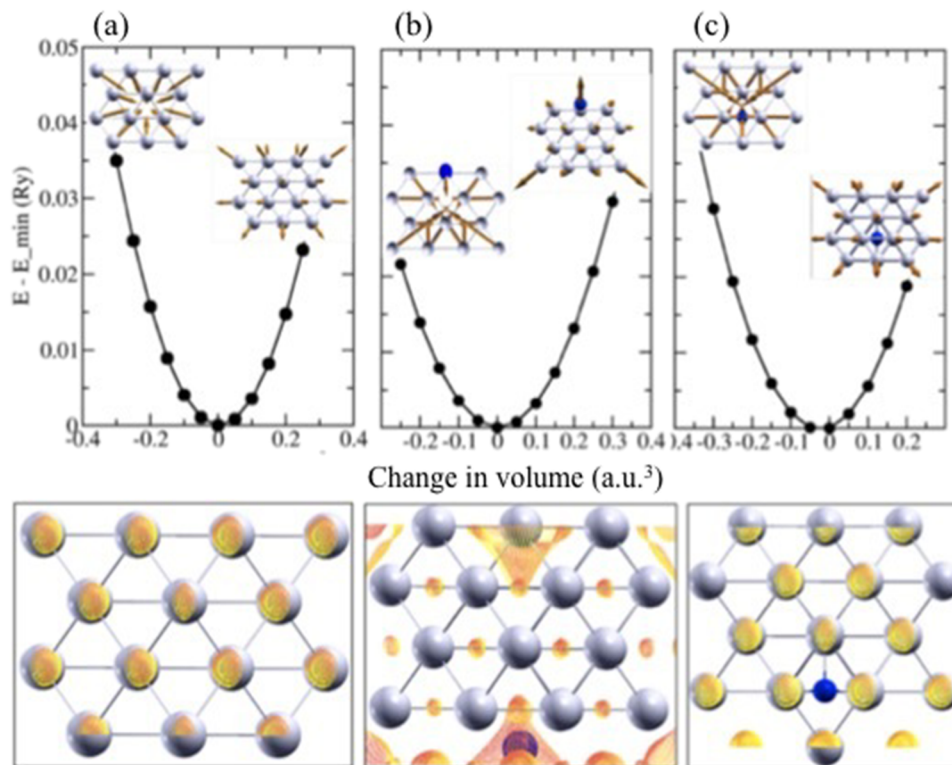
Raman spectra (lower panel of Fig. 1) shows a distinct G-peak ( $1600\text{ cm}^{-1}$ ) and D-peak ( $1290\text{ cm}^{-1}$ ) compared to the Raman spectra of the control sample with no carbon. This is a clear indication of the presence of graphitic carbon in Al. Iftekar Jaim *et al.* studied the presence of epitaxial graphene on the Al surface.<sup>5</sup> In this work, we study the effect of isolated carbon scatterers and planar carbon networks on the structure and bulk modulus of Al-C composites.

Figure 2 shows the total energy as a function of volume for (a) pristine Al and (b)  $C_1^0$  (purely substitutional doped) and

**TABLE I.** Structural information and the bulk modulus of Al-C composites (a: lattice constant; B: bulk modulus).

Configuration	Composition	$a$ (Å)	$B$ (GPa)
$C_0^0$	$\text{Al}_{32}\text{C}_0$	8.08	77.3
$C_1^0$	$\text{Al}_{31}\text{C}_1$	8.07	70.6
$C_0^1$	$\text{Al}_{32}\text{C}_1$	8.106	79.9
$C_0^2$	$\text{Al}_{32}\text{C}_2$	8.13	84.2
$C_2^0$ (a)	$\text{Al}_{30}\text{C}_2$	8.06	61.2
$C_2^0$ (b)	$\text{Al}_{30}\text{C}_2$	8.11	71.2
$C_1^1$	$\text{Al}_{31}\text{C}_2$	8.04	78.9
$C_6^0$ (a)	$\text{Al}_{32}\text{C}_6$	8.22	93.8
$C_6^0$ (b)	$\text{Al}_{32}\text{C}_6$	8.42	63.4
$C_0^{18}$	$\text{Al}_{32}\text{C}_6$	8.38	94.4

(c)  $C_0^1$  (purely interstitial doped) configurations. In the substitutional doped configuration,  $C_1^0$  [shown in Fig. 2(b)], one out of 32 C atoms in the supercell is doped with a C atom, whereas an additional C atom takes one out of eight empty body centered positions in the purely interstitial configuration,  $C_0^1$  [shown in Fig. 2(c)]. The lattice constant and the bulk modulus of pristine Al are 4.04 Å and 77.3 GPa, respectively, which are in agreement with the previous theoretical and experimental results.<sup>13,14</sup> The change in equilibrium lattice constants of the  $C_1^0$  and  $C_0^1$  configurations is  $-0.12\%$  and



**FIG. 2.** Upper panels show the total energy as a function of volume for (a) pristine Al and (b)  $C_1^0$  (purely substitutional doped) and (c)  $C_0^1$  (purely interstitial doped) configurations, with their charge density shown in the corresponding lower panels.

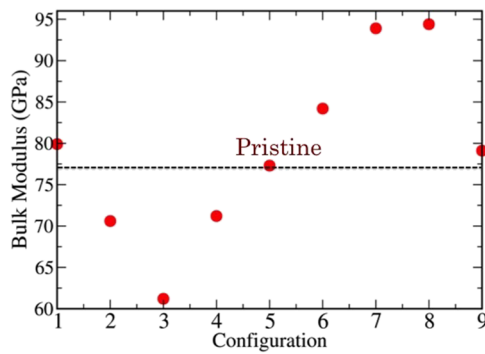


**FIG. 3.** Theoretically calculated bulk modulus of Al-C configurations [1:  $C_0^1$ , 2:  $C_1^0$ , 3:  $C_2^0(a)$ , 4:  $C_2^0(b)$ , 6:  $C_0^6$ , 7:  $C_0^6(a)$ , 8:  $C_0^{18}$ , and 9:  $C_1^1$ ].

0.32%, respectively (Table I). In the energy–volume curves shown in Fig. 2, the volume-axis is centered at the equilibrium volume, and the zero of the energy-axis is the equilibrium energy of each configuration.

The lower panel of Fig. 2 shows the charge density of each configuration. The pristine configuration is a uniformly distributed delocalized charge configuration. When a single Al atom is substituted by a C atom, localization of charge density is observed as shown in panel (b) of Fig. 2, which results in an 8.6% decrease in the bulk modulus, to 70.6 GPa. Purely interstitial substitutions to the Al crystal cause only a slight disturbance to the charge density; thus, the bulk modulus increases by 3.3%, to 79.9 GPa. The localization of charge in the substitutional doped configuration ( $C_1^0$ ) and delocalized charge distribution of the interstitial doped configuration explain this behavior, which is in agreement with the previously reported studies of elastic properties in other materials.<sup>15</sup>

In order to understand the variation in the bulk modulus from the experimental study [shown in Fig. 1(a)], we calculated the bulk moduli of seven other Al-C composite configurations. The chemical compositions, lattice constants, and the bulk moduli of these configurations are shown in Table I.

As shown in Table I, the bulk moduli of Al-C composites vary between 60 and 100 GPa for those considered configurations (Fig. 3), which are described in detail below.  $C_0^2$  has two substitutional atoms,

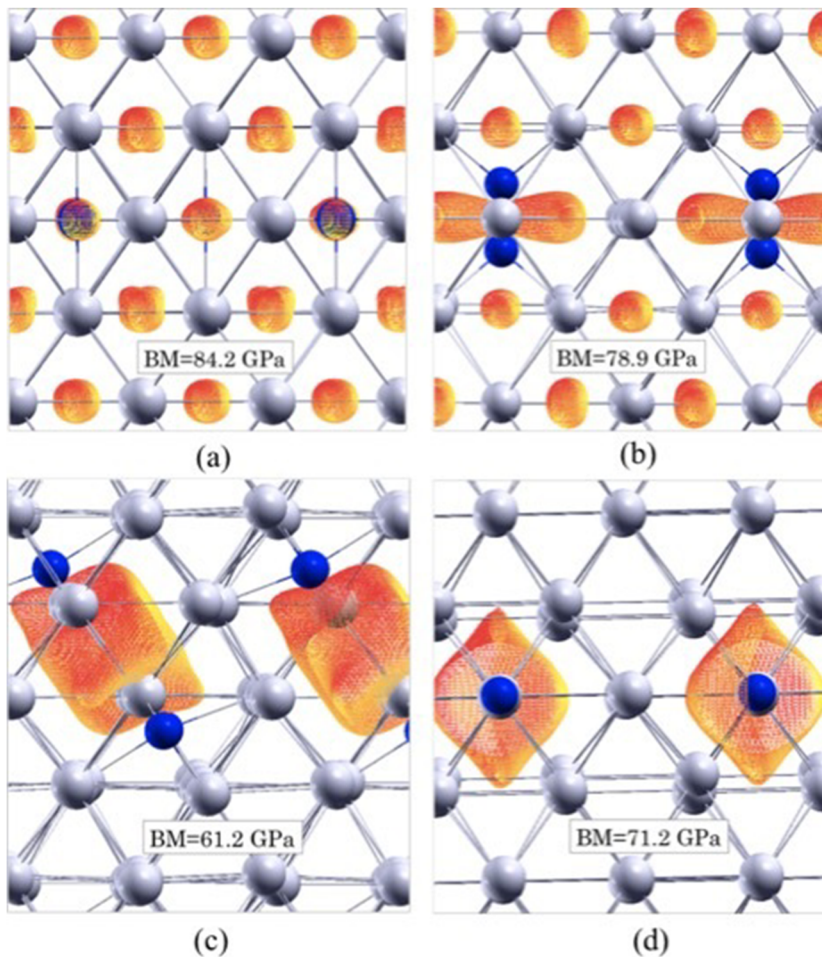


**FIG. 4.** Charge density distribution of (a)  $C_0^2$ , (b)  $C_1^1$ , (c)  $C_2^0(a)$ , and (d)  $C_2^0(b)$  configurations.

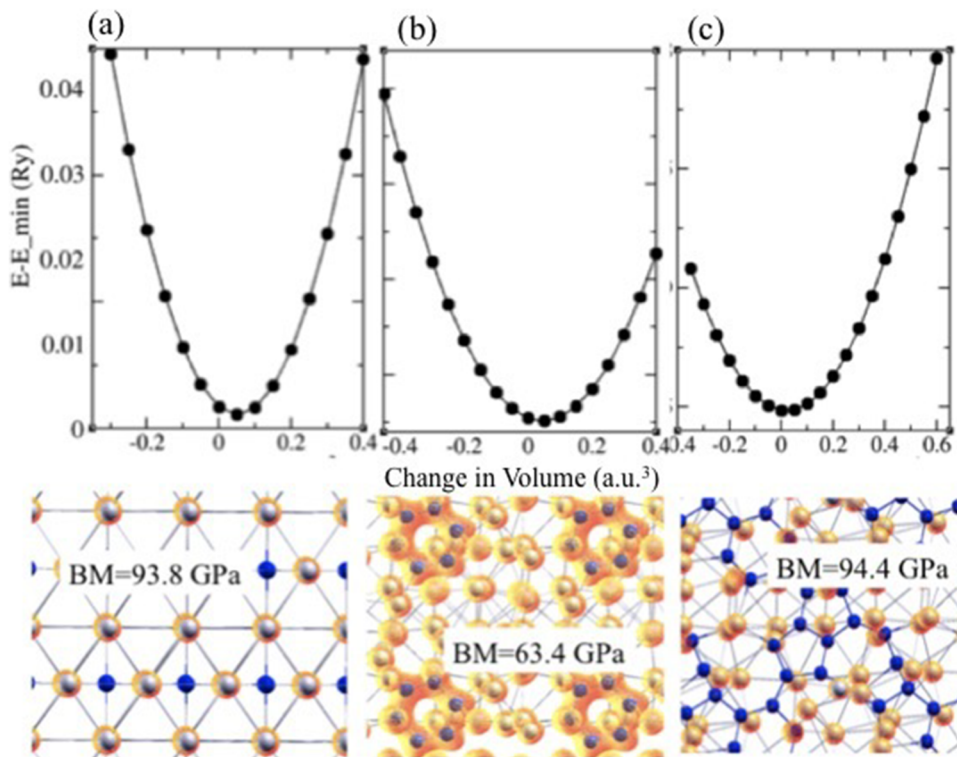


FIG. 5. Charge density distribution of (a)  $C_0^6$ (a), (b)  $C_0^6$ (b), and (c)  $C_0^{18}$  configurations.

with the chemical composition  $Al_{32}C_2$  showing  $B = 84.2$  GPa. This structure shows a delocalized charge distribution. The structure  $C_1^1$  with the chemical composition  $Al_{31}C_1$  has one substituted C atom and one interstitial C atom. This structure shows slight localization of charge density compared to  $C_0^2$ . The  $C_1^1$  structure shows  $B = 78.9$  GPa. Both  $C_2^0$ (a) and  $C_2^0$ (b) have the same chemical composition  $Al_{30}C_2$ , that is, with two substituted C atoms. The relative positions of the defects are different in the two structures. Both structures show localized charge distribution, as shown in Figs. 4(c) and 4(d) with  $B = 61.2$  and  $71.2$  GPa, respectively.

We have performed calculations on three additional Al-C composites to understand the behavior of C rings in the Al lattice. The first two structures have the chemical composition  $Al_{32}C_6$ , both with the configuration  $C_0^6$ , i.e., all six C atoms take interstitial positions. Our results show  $B = 63.4$  GPa for  $C_0^6$ (a) with a ring-shaped carbon cluster and  $B = 93.8$  GPa for  $C_0^6$ (b) with a pattern of scatterers,

which causes less disturbance to the charge distribution, as shown in Fig. 5. Our calculations show that the ring-shaped cluster is more energetically favorable than the isolated scatterers. A ring-shaped carbon cluster in the Al matrix with the composition  $Al_{26}C_{18}$  shows a higher bulk modulus of 94.4 GPa. The extended C-network supports the localized charge distribution less, which results in a higher bulk modulus.

Atomic displacements corresponding to the highest frequency phonons at the gamma point for the three configurations are shown in Fig. 6. When there are carbon scatterers [such as in configurations (a)  $C_0^1$  and (b)  $C_0^6$ (a)], the highest vibrational frequency is around  $600\text{ cm}^{-1}$ , and the corresponding atomic displacement shows a vibration of C atoms along with the Al-matrix, as shown in Figs. 6(a) and 6(b). In the  $C_0^{18}$  configuration, the highest vibrational frequency is shown at  $1357\text{ cm}^{-1}$ , and the corresponding atomic displacements are solely restricted to the plane of honey-

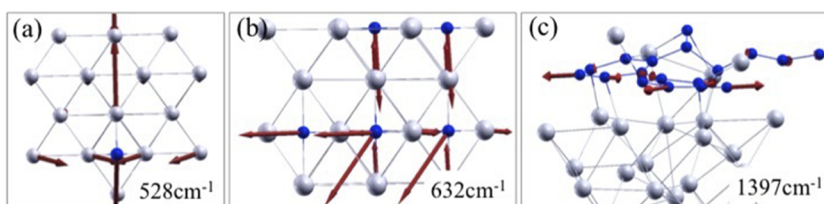


FIG. 6. Atomic displacement pattern corresponding to the highest frequency of gamma-point phonons: (a)  $C_0^1$ , (b)  $C_0^6$ (a), and (c)  $C_0^{18}$  configurations.

combs in the C-cluster, in addition, it has similarities to the D-peak observed at  $1290\text{ cm}^{-1}$  for graphene,<sup>16</sup> which further confirms our conclusion on formation of  $sp^2$  hybridized carbon clusters in the Al-matrix.

Our work shows that graphitic carbon can form in the Al matrix by the hot isostatic process growth approach. Our calculations also show that ring-shaped structures are energetically more favorable than isolated scatterers. However, even the small rings or isolated scatterers can reduce the bulk modulus if defects are formed at the localized charge centers in the Al matrix. Extended ring-shaped graphitic carbon clusters can increase the bulk modulus of Al.

This work was partially supported by an NSF grant (Award No. 2138459) and the NSF DMR and DoD Assure REU Program (Award No. 1757954). The authors would like to thank Southern Illinois University for providing the computer facilities.

## AUTHOR DECLARATIONS

### Conflict of Interest

The authors have no conflicts to disclose.

### Author Contributions

**Hansika I. Sirikumara:** Writing – original draft (equal); Writing – review & editing (equal). **Wilson Rativa-Parada:** Writing – review & editing (supporting). **Robinson Karunanithy:** Methodology (supporting). **Poopalasingam Sivakumar:** Methodology (supporting). **Sabrina Nilufar:** Methodology (supporting); Writing – review & editing (supporting). **Thushari Jayasekera:** Writing – review & editing (supporting).

### DATA AVAILABILITY

The data that support the findings of this study are available within the article.

## REFERENCES

- <sup>1</sup>Z. Wang, R. T. Qu, S. Scudino, B. A. Sun, K. G. Prashanth, D. V. Louzguine-Luzgin, M. W. Chen, Z. F. Zhang, and J. Eckert, “Hybrid nanostructured aluminum alloy with super-high strength,” *NPG Asia Mater.* **7**, e229 (2015).
- <sup>2</sup>N. Chawla and Y.-L. Shen, “Mechanical behavior of particle reinforced metal matrix composites,” *Adv. Eng. Mater.* **3**, 357–370 (2001).
- <sup>3</sup>C. Suryanarayana and N. Al-Aqeeli, “Mechanically alloyed nanocomposites,” *Prog. Mater. Sci.* **58**, 383–502 (2013).
- <sup>4</sup>C. A. Smith, *Discontinuous Reinforcements for Metal-Matrix Composites* (ASM International, Materials Park, OH, 2001), pp. 51–55.
- <sup>5</sup>H. M. I. Jaim, R. A. Isaacs, S. N. Rashkeev, M. Kuklja, D. P. Cole, M. C. LeMieux, I. Jasiuk, S. Nilufar, and L. G. Salamanca-Riba, “ $Sp^2$  carbon embedded in Al-6061 and Al-7075 alloys in the form of crystalline graphene nanoribbons,” *Carbon* **107**, 56–66 (2016).
- <sup>6</sup>B. Sahoo, J. Joseph, A. Sharma, and J. Paul, “Surface modification of aluminium by graphene impregnation,” *Mater. Des.* **116**, 51–64 (2017).
- <sup>7</sup>S. Zhang, D. He, P. Huang, and F. Wang, “Moiré pattern at graphene/Al (111) interface: Experiment and simulation,” *Mater. Des.* **201**, 109509 (2021).
- <sup>8</sup>A. J. Jackson, J. M. Skelton, C. H. Hendon, K. T. Butler, and A. Walsh, “Crystal structure optimisation using an auxiliary equation of state,” *J. Chem. Phys.* **143**, 184101 (2015).
- <sup>9</sup>F. D. Murnaghan, “The compressibility of media under extreme pressures,” *Proc. Natl. Acad. Sci. U. S. A.* **30**, 244–247 (1944).
- <sup>10</sup>F. Birch, “Finite elastic strain of cubic crystals,” *Phys. Rev.* **71**, 809 (1947).
- <sup>11</sup>P. Giannozzi, S. Baroni, N. Bonini, M. Calandra, R. Car, C. Cavazzoni, D. Ceresoli, G. L. Chiarotti, M. Cococcioni, I. Dabo, A. Dal Corso, S. de Gironcoli, S. Fabris, G. Fratesi, R. Gebauer, U. Gerstmann, C. Gougoussis, A. Kokalj, M. Lazzeri, L. Martin-Samos, N. Marzari, F. Mauri, R. Mazzarello, S. Paolini, A. Pasquarello, L. Paulatto, C. Sbraccia, S. Scandolo, G. Sclauzero, A. P. Seitsonen, A. Smogunov, P. Umari, and R. M. Wentzcovitch, “QUANTUM ESPRESSO: A modular and open-source software project for quantum simulations of materials,” *J. Phys.: Condens. Matter* **21**, 395502 (2009).
- <sup>12</sup>J. P. Perdew, K. Burke, and M. Ernzerhof, “Generalized gradient approximation made simple,” *Phys. Rev. Lett.* **77**, 3865 (1996).
- <sup>13</sup>P. Jacobs, Y. F. Zhukovskii, Y. Matrikov, and Y. N. Shunin, “Bulk and surface properties of metallic aluminium: DFT simulations,” *Comput. Modell. New Technol.* **6**, 7–28 (2002).
- <sup>14</sup>W. Li and T. Wang, “*Ab initio* investigation of the elasticity and stability of aluminium,” *J. Phys.: Condens. Matter* **10**, 9889 (1998).
- <sup>15</sup>M. Woodcox, J. Young, and M. Smeu, “*Ab initio* investigation of the elastic properties of bismuth-based alloys,” *Phys. Rev. B* **100**, 104105 (2019).
- <sup>16</sup>J. Pešić, V. Damljanović, R. Gajić, K. Hingerl, and M. Belić, “Density functional theory study of phonons in graphene doped with Li, Ca and Ba,” *Europhys. Lett.* **112**, 67006 (2016).